Intermediate models in nonlinear optics.

Thierry Colin[(1)], Gérard Gallice[(2)] and Karen Laurioux[(1,2)]
[(1)] MAB, Université Bordeaux 1 et CNRS UMR 5466, 351 cours de la libération, 33405 Talence cedex, France.
[(2)] SIS, CEA CESTA, BP2, 33114 Le Barp, France.
colin@math.u-bordeaux.fr
gallice@cea.fr

Abstract: In this paper, new models are derived for laser propagation in a nonlinear medium. These models are intermediate between nonlinear Maxwell systems and nonlinear Schrödinger equations and are exact in linear cases. We prove rigorous error estimates for a generic class of systems. In the last section, we perform numerical tests in order to investigate the numerical effectivity of the bounds given by the theorem. We compare for a particular nonlinear system the exact solutions and the approximate solutions given by our new model. It is shown that the new models behave as predicted by the theorem but are even better in some cases.

1 Introduction

1.1 Motivations

The aim of this paper is to propose new models for the simulation of the propagation of laser pulses in a nonlinear medium. The wavelength associated to a pulse is usually near the micrometer (10^{-6}m) while the length of the pulse can be of order 100 micrometers for ultrashort pulses (10^{-4}m) or of the order of the meter. We are concerned with propagation on distances of order of the millimeter (for crystals) or of hundred of meters (for propagation in gas). From the temporal point of view, the frequency of a pulse is $10^{15}s^{-1}$, its duration can be of the order of the picoseconds ($10^{-12}s$) or of 10 nanoseconds ($10^{-8}s$). The duration of propagation can be $10^{-11}s$ for crystals or $10^{-6}s$ for gas. The width of the beam can be of order of a fraction of millimeter to a few centimeters. Therefore, one has to handle 3D processes involving several orders of magnitude. It is not possible to propose direct simulations for all these situations. Usually, the so-called paraxial approximation or envelope approximation are used. This approximation relies on the fact that the electric field has the form of a plane wave multiplied by an envelope, namely $e^{i(kz-\omega t)}\mathcal{E}(t,x,y,z)$ where $t \geq 0$ is the time, $(x,y,z) \in \mathbb{R}^3$ are the spatial variables, k is the wave number and ω the frequency. With these notations, the slowly varying envelope approximation can be expressed by the following set of inequalities:

$$|\partial_t \mathcal{E}| << \omega|\mathcal{E}|, \quad |\partial_x \mathcal{E}| << k|\mathcal{E}|, \quad |\partial_y \mathcal{E}| << k|\mathcal{E}|, \quad |\partial_z \mathcal{E}| << k|\mathcal{E}|.$$

Using these inequalities, one obtains approximate equations satisfied by $\mathcal{E}$. These equations can be nonlinear transport equations at the group velocity

(for frequency doubling in the phase-matching case in a crystal) or nonlinear Schrödinger equations (in a Kerr medium) or Schrödinger-Bloch equations (in a gas) ... We refer to general textbook of physics ([8], [18] for instance) for a precise physical description. Here, we will address cases where the validity of the paraxial approximation is not so clear. Physically, this can occur when the pulse goes through a diffraction web or when the pulse is "chirped" in order to have a large spectral width. We want to propose alternative intermediate models that are more precise than the usual Schrödinger-like equation but less expensive to compute numerically than the full Maxwell equations. These intermediate models are obtained in the same spirit as the long wave systems for water waves of [6] or [7]. For direct simulations on nonlinear Maxwell systems, see [5] and references therein. See also [3] for cases with non planar phases. In order to introduce our notations, let us recall that a standard model for propagation of a beam in a Kerr medium is the Maxwell-Lorentz system which has the non-dimensional form:

$$\begin{cases} \partial_t B + \text{curl } E = 0, \\ \partial_t E - \text{curl } B = -\partial_t P, \\ \partial_t^2 P - \dfrac{1}{\varepsilon^2}(E - P) = \dfrac{1}{\varepsilon}|P|^2 P, \end{cases} \tag{1.1}$$

where (E, B) is the electromagnetic field, P is the polarization. Introducing $Q = \varepsilon \partial_t P$, this system becomes:

$$\begin{cases} \partial_t B + \text{curl } E = 0, \\ \partial_t E - \text{curl } B = -\dfrac{Q}{\varepsilon}, \\ \partial_t Q - \dfrac{1}{\varepsilon}(E - P) = |P|^2 P, \\ \partial_t P - \dfrac{1}{\varepsilon} Q = 0. \end{cases} \tag{1.2}$$

For propagation in gas, one can use the two-level Maxwell-Bloch system:

$$\begin{cases} \partial_t E - \text{curl } B + \partial_t P = 0, \\ \partial_t B + \text{curl } E = 0, \\ P = \text{Re}(c_1 c_2^*) u, \end{cases} \tag{1.3}$$

where c_1 and c_2 are the complex representations of the populations in each level (c_2^* denotes the complex conjugate of c_2) and u a fixed vector corresponding to the direction of propagation. Level 1 corresponds to the fundamental state,

while level 2 corresponds to the excited state. The evolution of c_1 and c_2 is given by the following set of ordinary differential equations which is derived from the Schrödinger equation of quantum mechanics [18]:

$$\begin{cases} i\partial_t c_1 = -\dfrac{E \cdot u c_2}{\varepsilon}, \\ \\ i\partial_t c_2 = \dfrac{1}{\varepsilon} c_2 - \dfrac{E \cdot u c_1}{\varepsilon}. \end{cases} \tag{1.4}$$

Introducing $\Lambda = c_1 c_2^*$ and $\tilde{N} = |c_1|^2 - |c_2|^2$ yields

$$\begin{cases} \partial_t \Lambda = \dfrac{i\Lambda}{\varepsilon} - \dfrac{iE \cdot u \tilde{N}}{\varepsilon}, \\ \\ \partial_t \tilde{N} = -\dfrac{2iE \cdot u(\Lambda - \Lambda^*)}{\varepsilon}. \end{cases} \tag{1.5}$$

Let $P = \mathrm{Re}(\Lambda)$, $Q = \mathrm{Im}(\Lambda)$ and $\tilde{N} = 1 - N$, we obtain

$$\begin{cases} \partial_t P = -\dfrac{1}{\varepsilon} Q, \\ \\ \partial_t Q = \dfrac{1}{\varepsilon} P - \dfrac{E \cdot u(1-N)}{\varepsilon}, \\ \\ \partial_t N = -\dfrac{4E \cdot uQ}{\varepsilon}. \end{cases} \tag{1.6}$$

Now we change all the unknows by a scaling factor $\sqrt{\varepsilon}$ and we consider a vectorial form of (1.6) without assuming that the electric filed is polarized along the unit vector u:

$$\begin{cases} \partial_t B + \mathrm{curl}\ E = 0, \\ \\ \partial_t E - \mathrm{curl}\ B = \dfrac{Q}{\varepsilon}, \\ \\ \partial_t Q + \dfrac{1}{\varepsilon}(E - P) = EN, \\ \\ \partial_t P + \dfrac{1}{\varepsilon} Q = 0, \\ \\ \partial_t N = -4E \cdot Q. \end{cases} \tag{1.7}$$

See [11] for a precise description of these models and the derivation of the non dimensional forms. See also [10] for the use of Maxwell-Bloch in a gas. Since the solutions are expected under the form of a plane wave multiplied by an envelope, usually the initial data is taken as being equal to

$$(E, B, P, Q)(t = 0, X) = e^{i\frac{k \cdot X}{\varepsilon}} (E_0, B_0, P_0, Q_0)(X) + c.c.$$

with $X = (x, y, z)$ and $k \in \mathbb{R}^3$. The notation *c.c.* means "complex conjugate ". For (1.7), one has moreover to take $N(t = 0, X) = 0$ since at the state of rest, all atoms are at level one and $c_1 = 1$ and $c_2 = 0$ which implies $N = 0$. Therefore the difficulties concerning the presence of different length scales for the propagation of the beam appears in (1.2) and (1.7) through the presence of terms of size $\frac{1}{\varepsilon}$ in the equations and also in the $e^{i\frac{k\cdot X}{\varepsilon}}$ in the initial data. These terms will create high frequencies (of order $\frac{1}{\varepsilon}$) in time. Moreover we will need to characterize the solution on short time scale ($O(1)$) or on long time scale ($O(\frac{1}{\varepsilon})$), that is on long or short distance. In order to give a synthetic presentation of these phenomenas, we introduce the following general class of systems (including (1.1) and (1.3)) that has been used in several works ([16], [15], [14], [9] ...):

$$\left(\partial_t + \sum_{j=1}^{n} A_j \partial_{x_j} + \frac{L_0}{\varepsilon}\right) u = f(u), \tag{1.8}$$

where matrices A_j are real symmetric, L_0 is skew-symmetric, f is a smooth nonlinear mapping and

$$u(t, X) : [0, T] \times \mathbb{R}^n \to \mathbb{R}^p, \quad X = (x_1, \cdots, x_n).$$

For the sake of simplicity, in this paper we will restrict ourselves to the case where $f(u)$ is an homogeneous polynomial of degree q. Of course all of the results can be extended to more general cases.

1.2 Some classical results of nonlinear geometrical optics.

We recall some tools of geometrical optics (see [14] for a more complete description). First we seek for plane wave solutions to the linear part of (3.1) that is

$$u = Fe^{\frac{i(k\cdot X - \omega t)}{\varepsilon}}, \tag{1.9}$$

where $F \in \mathbb{C}^p$ is a constant and $k = (k_1, \cdots, k_n) \in \mathbb{R}^n$. Such a plane wave is a solution to

$$\left(\partial_t + \sum_{j=1}^{n} A_j \partial_{x_j} + \frac{L_0}{\varepsilon}\right) u = 0, \tag{1.10}$$

if and only if

$$\left(-i\omega I_d + i\sum_{j=1}^{n} A_j k_j + L_0\right) F = 0, \tag{1.11}$$

where I_d denotes the identity matrix.
System (1.11) has a nontrivial solution if and only if

$$det\left(-i\omega I_d + i\sum_{j=1}^{n} A_j k_j + L_0\right) = 0, \tag{1.12}$$

which is the dispersion relation. Note that matrix $i\sum_{j=1}^{n} A_j k_j + L_0$ is skew-adjoint, therefore the solutions ω are real and the solutions $i\omega$ are the eigenvalues of $i\sum_{j=1}^{n} A_j k_j + L_0$. Moreover the eigenspaces are orthogonal. We denote by $\Pi(\omega, k)$ (or simply by $\Pi(k)$ if no confusion is possible) the orthogonal projector onto $Ker\left(-i\omega I_d + i\sum_{j=1}^{n} A_j k_j + L_0\right)$. We also give the following definition:

Definition 1.1 *The characteristic variety $\mathcal{C}_{\mathcal{L}}$ of the operator $\mathcal{L}(\partial_t, \partial_X) = \partial_t + A(\partial_X) + L_0 := \partial_t + \sum_{j=1}^{n} A_j \partial_{x_j} + L_0$ is the set*

$$\mathcal{C}_{\mathcal{L}} = \{(\tau, \xi) \in \mathbb{R} \times \mathbb{R}^n \text{ such that } det(-i\tau I_d + iA(\xi) + L_0) = 0\}.$$

Now, coming back to the nonlinear system (1.8), one tries to solve

$$\left(\partial_t + \sum_{j=1}^{n} A_j \partial_{x_j} + \frac{L_0}{\varepsilon}\right) u = f(u).$$

For a given $k \in \mathbb{R}^n$, we select a frequency ω. The way we solve this problem is the following one. We look for u in the form

$$u(t, X) = \mathcal{U}(\frac{k \cdot X - \omega t}{\varepsilon}, t, X),$$

where $\theta \mapsto \mathcal{U}(\theta, t, X)$ is $2\pi-$periodic. Of course this is not enough in order to define completely function $\mathcal{U}$. We see that $\mathcal{U}$ satisfies the following singular equation:

$$\left(\partial_t + A(\partial_X) + \frac{1}{\varepsilon}\left(-\omega\partial_\theta + A(k)\partial_\theta + L_0\right)\right)\mathcal{U} = f(\mathcal{U}), \text{ for all } t \in [0, T], \tag{1.13}$$

for all $X \in \mathbb{R}^n$ and for $\theta = \dfrac{k \cdot X - \omega t}{\varepsilon}$. At this stage, function $\mathcal{U}$ is not well defined since it satisfies (1.13) only for $\theta = \dfrac{k \cdot X - \omega t}{\varepsilon}$. In order to give a correct definition, we impose that $\mathcal{U}$ satisfies (1.13) for all $t \in [0, T]$, $X \in \mathbb{R}^N$ and for $\theta \in \mathbb{T}$ where $\mathbb{T}$ denotes the usual one-dimensional torus. We make the following generic hypothesis.

Hypothesis 1. *(k, ω) is a regular point of $\mathcal{C}_L$ (that is the multiplicity of the eigenvalue $\lambda_j(\xi)$ such that $\lambda_j(k) = \omega$ is constant in a neighborhood of $\xi = k$).*

Hypothesis 2. *$(pk, p\omega) \notin \mathcal{C}_L$ for all integer $p \leq q$, where q is the degree of the nonlinearity f.*

Note that hypothesis 2 is not necessary; we could replace it by the strong finiteness hypothesis as in [12]. One then can construct an approximate solution for u as follows. Let $\mathcal{U}_0$ be the solution to

$$\begin{cases} \partial_t \mathcal{U}_0 + \omega'(k) \cdot \partial_X \mathcal{U}_0 = \Pi(k) C_1 \left(f(\Pi(k)\mathcal{U}_0 e^{i\theta} + c.c.) \right), \\ \\ \mathcal{U}_0(t=0,X) = \mathcal{U}_0(X). \end{cases} \tag{1.14}$$

where $C_q\left(F(\theta)\right)$ denotes the q^{th} Fourier coefficient of $\theta \mapsto F(\theta)$:

$$C_q\left(F(\theta)\right) = \frac{1}{2\pi} \int_0^{2\pi} F(\theta) e^{iq\theta} d\theta.$$

One then shows:

Theorem 1.1 *Let $u_0 \in H^s(\mathbb{R}^n)$ (s large enough) such that $\Pi(k)u_0 = u_0$. There exists a unique $\mathcal{U}^\varepsilon(\theta,t,X)$ solution to the singular equation (1.13) such that $\mathcal{U}^\varepsilon(\theta,0,X) = (e^{i\theta}u_0 + c.c.)$ is defined on $[0,T]$ and*

$$\left| \mathcal{U}^\varepsilon(\theta,t,X) - (\mathcal{U}_0(t,X)e^{i\theta} + c.c.) \right|_{L^\infty_t(0,T;H^s_{\theta,X})} \leq C_0 \varepsilon.$$

It follows that there exists a solution $u^\varepsilon(t,X)$ to (1.8) such that $u^\varepsilon(0,X) = \left(e^{\frac{ik\cdot X}{\varepsilon}} u_0(X) + c.c. \right)$ and

$$\left| u^\varepsilon(t,X) - (\mathcal{U}_0(t,X) e^{i\frac{k\cdot X - \omega t}{\varepsilon}} + c.c.) \right|_{L^\infty([0,T]\times\mathbb{R}^n)} \leq C_0 \varepsilon.$$

This regime is called geometrical optics. For solutions on long time scale of size $O(\frac{1}{\varepsilon})$, diffractive effects are important and we have to give another expansion. We look for a solution of (1.8) satisfying

$$u(t=0,X) = \varepsilon^{1/(q-1)} \left(e^{\frac{ik\cdot X}{\varepsilon}} u_0(X) + c.c. \right).$$

Let us recall that q is the order of the nonlinearity. In order to explain briefly why this scaling $\varepsilon^{1/(q-1)}$ is relevant, let us consider the ordinary differential equation $y' = y^q$. An initial data of size $\varepsilon^{1/(q-1)}$ will lead to a solution of the same size $y(t) = \varepsilon^{1/(q-1)} z(t)$. Then function $z(t)$ satisfies

$$z'(t) = \varepsilon^{q/(q-1)} \varepsilon^{-1/(q-1)} z^q = \varepsilon z(t)^q$$

and $z(t)$ is therefore defined on a time interval of size $O(\frac{1}{\varepsilon})$.
The solution u is sought in the form

$$u(t,X) = \mathcal{U}\left(\frac{k\cdot X - \omega t}{\varepsilon}, X - \omega'(k)t, \varepsilon t \right)$$

where $\theta \mapsto \mathcal{U}(\theta, X, \tau)$ is defined on $\mathbb{T} \times \mathbb{R}^n \times [0, T]$. This will lead to a solution to (1.8) defined on $[0, \frac{T}{\varepsilon}]$. $\mathcal{U}$ then satisfies

$$\left(\varepsilon\partial_\tau + (-\omega'(k)\partial_X + A(\partial_X)) + \frac{1}{\varepsilon}\left(-\omega\partial_\theta + A(k)\partial_\theta + L_0\right)\right)\mathcal{U} = f(\mathcal{U}), \quad (1.15)$$

with

$$\mathcal{U}(\theta, t = 0, X) = \varepsilon^{1/(q-1)}\left(e^{i\theta}u_0(x) + c.c.\right).$$

Let $\mathcal{V}_0$ be the solution to the following nonlinear Schrödinger equation:

$$\partial_\tau \mathcal{V}_0 + i\frac{\omega''(k)}{2}(\partial_X, \partial_X)\mathcal{V}_0 = \Pi(k)C_1\left(f(\Pi(k)\mathcal{V}_0 e^{i\theta} + c.c.)\right), \quad (1.16)$$

with $\mathcal{V}_0(\tau = 0, X) = u_0(X)$.

Theorem 1.2 *Let $u_0 \in H^s(\mathbb{R}^n)$ (s large enough) such that $\Pi(k)u_0 = u_0$. There exists a unique $\mathcal{V}^\varepsilon(\theta, X, \tau)$ solution to the singular equation (1.15) such that $\mathcal{V}^\varepsilon(\theta, X, 0) = \varepsilon^{1/(q-1)}(e^{i\theta}u_0 + c.c.)$ defined on $[0, T]$ and*

$$\left|\frac{1}{\varepsilon^{1/(q-1)}}\mathcal{V}^\varepsilon(\theta, X, \tau) - (\mathcal{V}_0(\tau, X)e^{i\theta} + c.c.)\right|_{L^\infty_\tau(0,T;H^s_{\theta,X})} \leq C_1\varepsilon.$$

As before, it follows that

$$\left|\frac{1}{\varepsilon^{1/(q-1)}}u^\varepsilon(t, X) - (\mathcal{V}_0(\varepsilon t, X - \omega'(k)t)e^{i\frac{k\cdot X - \omega t}{\varepsilon}} + c.c.)\right|_{L^\infty([0,T]\times\mathbb{R}^n)} \leq C\varepsilon.$$

Of course, from the computational point of view, it is much easier to find low frequency solutions to (1.14) or (1.16) on $[0, T] \times \mathbb{R}^n$ than oscillatory solutions of (1.8) on $[0, \frac{T}{\varepsilon}] \times \mathbb{R}^n$. Indeed the frequencies in time and space that are relevant for the solution of (1.8) are of size $O(\frac{1}{\varepsilon})$. Therefore, the time and space steps used in any numerical method have to be small compared to ε. This gives a number of points (in space) that has to be large compared to $O(\frac{1}{\varepsilon})$ and a number of time steps large compared to $O(\frac{1}{\varepsilon})$. For (1.14) or (1.16), the frequencies are $O(1)$ and the time or space steps have only to be small with respect to 1. Moreover, while (1.8) has to be solved in the diffractive regime on long time intervals $[0, \frac{T}{\varepsilon}]$, equation (1.16) has to be solved on $[0, T]$ only, which decreases the number of time steps. This is why (1.14) or (1.16) are used in practical applications [17].

1.3 Limitations of the models.

In some applications (ultrashort pulses), one can have to handle cases where ε is small, but not very small ($\varepsilon \sim 10^{-2}$). The error estimates given by the above results are not very precise especially when the constants C_0 and C_1 (depending at least of the H^s norm of the initial data) are large. These constants can be large when the initial data has rapid variations and this is the case for short pulses or for pulses with a quite large spectrum. This configuration arises when the laser beam propagates through a diffraction web. We give a numerical example below. Let us consider the simplified system:

$$\partial_t \begin{pmatrix} u \\ v \end{pmatrix} + \partial_x \begin{pmatrix} v \\ u \end{pmatrix} + \frac{1}{\varepsilon} \begin{pmatrix} -v \\ u \end{pmatrix} = \begin{pmatrix} -(u^2+v^2)v \\ (u^2+v^2)u \end{pmatrix}, \tag{1.17}$$

with

$$\begin{pmatrix} u_0 \\ v_0 \end{pmatrix} = \varepsilon^{1/2} e^{i\frac{kx}{\varepsilon}} \begin{pmatrix} 1 \\ \frac{-ik+1}{i\omega} \end{pmatrix} a(x) + c.c., \quad x \in [0,1],$$

where $\omega = \sqrt{1+k^2}$. The function $a(x)$ is given by

$$a(x) = e^{-75(x-1/2)^2} e^{i15\cos(15x)}.$$

We make a simulation as described in the last section with $\varepsilon = 10^{-2}$ on $t \in [0, 50]$. The solution to (1.17) at time $t = 50$ is given on figure 1 and the solution given by the nonlinear Schrödinger equation (1.16) on figure 2. They have nothing in common and the relative error in L^2 norm is 1.4 as indicated in section 3.3.2. For practical use, O. Morice [17] has already introduced some modification of the linear Schrödinger equation in order to take into account higher-order diffraction effects. Other tentatives has been done by D. Alterman and J. Rauch [1], Schäfer and Wayne [19] and [2] for ultra-short pulses. In all these contributions, the authors obtain linear equation because in a context of pulses with large spectrum, it can be shown that the nonlinear effects are less important than usually see ([1] and [2]). Nevertheless, from the physical point of view, it is impossible to neglect nonlinear effects. We therefore need to construct new models that will be exact in the linear case, but that take into account the nonlinear effects and that are not numerically stiff.

This paper is organized as follows. In section 2, we introduce our new models and prove the main result. In section 3, we present some numerical results in order to illustrate our error bounds and also to investigate the numerical effectivity of our model.

2 New intermediate models.

2.1 Formal obtaining of the models.

We restrict ourselves to geometrical optics regime. We go back to the singular equation (1.13). For $\xi \in \mathbb{R}^n$, let us introduce the following spectral decomposition of the matrix $iA(\xi) + L_0$:

$$iA(\xi) + L_0 = \sum_{j=1}^{m} i\lambda_j(\xi)\Pi_j(\xi), \tag{2.1}$$

where m denotes the number of distinct eigenvalues of $iA(\xi) + L_0$. We have implicitly used the following assumption:

Hypothesis 3. *There exists m continuous functions $\xi \mapsto \lambda_j(\xi)$ defining a global parametrization of the characteristic variety C_L.*

Of course the functions $\xi \mapsto \Pi_j(\xi)$ are not necessary continuous at the points ξ_0 where there exists j_1 and j_2 such that $\lambda_{j_1}(\xi_0) = \lambda_{j_2}(\xi_0)$. However, since the projector $\Pi_j(\xi)$ are orthogonal projectors, the functions $\xi \mapsto \Pi_j(\xi)$ are bounded. Let us now fix a vector $k \in \mathbb{R}^n$ and take $\omega = \lambda_{l_0}(k)$ one eigenvalue of $iA(\xi) + L_0$ for some $l_0 \in \{1, \cdots, m\}$. In order to simplify the notations, we take $l_0 = 1$. (k, ω) will be the main frequencies of the solution described in the introduction.

Hypothesis 4. *There exists a neighborhood V of k such that for all $\xi \in V$ and for all integer $j \geq 2$*

$$\lambda_j(\xi) \neq \lambda_1(\xi).$$

From now on, we use the usual notations $D_\theta = \dfrac{\partial_\theta}{i}$, $D_X = \dfrac{\partial_X}{i}$. Then, equation (1.13) reads:

$$\left(\partial_t + \frac{1}{\varepsilon}\left(-i\omega D_\theta + iA(kD_\theta + \varepsilon D_X) + L_0\right)\right)\mathcal{U}^\varepsilon = f(\mathcal{U}^\varepsilon).$$

Using (2.1), we get

$$\begin{aligned}\left(\partial_t + \frac{1}{\varepsilon}\left(-i\omega D_\theta + i\lambda_j(kD_\theta + \varepsilon D_X)\right)\right)\Pi_j(kD_\theta + \varepsilon D_X)\mathcal{U}^\varepsilon \\ = \Pi_j(kD_\theta + \varepsilon D_X)f(\mathcal{U}^\varepsilon), \quad j = 1 \text{ to } m.\end{aligned} \tag{2.2}$$

The first model that we introduce relies on the following idea: we want to obtain a model that is exact for the linear regime ($f \equiv 0$) and the best possible for the nonlinear one. Moreover, one starts with initial data that are polarized on the first eigenspace that is

$$\Pi_1(kD_\theta + \varepsilon D_X)\mathcal{U}^\varepsilon(t = 0) = \mathcal{U}^\varepsilon(t = 0).$$

We now make the following hypothesis

Hypothesis 5. *If $m \in \mathbb{Z}$, $j = 1$ to m, then*

$$\lambda_j(mk) = m\omega \Rightarrow j = 1 \text{ and } m = \pm 1.$$

One can modify the model obtained below if this assumption is not satisfied. In fact a generalized assumption is the strong finiteness hypothesis introduced in [12]:

Hypothesis 5'. *The set* $\{m \in \mathbb{Z}$ *such that there exists* j *satisfying* $\lambda_j(mk) = m\omega$ $\}$ *is finite.*

However for the sake of simplicity, we will restrict in this work to Hypothesis 5. Under the hypothesis 5, the spectrum of the solution will be mainly supported by the first sheet of the characteristic variety. That is for all time, we will have $\Pi_1(kD_\theta + \varepsilon D_X)\mathcal{U}^\varepsilon(t) \approx \mathcal{U}^\varepsilon(t)$. We therefore introduce $\mathcal{V}^\varepsilon$ the solution to

$$\begin{aligned}\left(\partial_t + \frac{1}{\varepsilon}\left(-i\omega D_\theta + i\lambda_1(kD_\theta + \varepsilon D_X)\right)\right)\Pi_1(kD_\theta + \varepsilon D_X)\mathcal{V}^\varepsilon \\ = \Pi_1(kD_\theta + \varepsilon D_X) f(\mathcal{V}^\varepsilon),\end{aligned} \tag{2.3}$$

and

$$\Pi_j(kD_\theta + \varepsilon D_X)\mathcal{V}^\varepsilon = 0 \text{ for } j \geq 2. \tag{2.4}$$

We expect $\mathcal{V}^\varepsilon$ to be a good approximation of $\mathcal{U}^\varepsilon$. For $s \in \mathbb{R}$ and $T > 0$ we denote by $X_T = L^\infty(0, T; H^s(\mathbb{R}^n_X \times \mathbb{T}_\theta))$. Our first result reads as follows.

Theorem 2.1 *Let us assume hypothesis 3, 4, 5 and let* $s > \dfrac{n+1}{2}$, $\alpha > 0$. *Let* $u_0(X) \in H^\sigma(\mathbb{R}^n)$ *(for* σ *large enough) satisfying*

$$\Pi_1(k + \varepsilon D_X)u_0(X) = u_0(X).$$

Then there exists $T > 0$ *(independent of* ε*) and* $\mathcal{U}^\varepsilon$, $\mathcal{V}^\varepsilon$ *respectively solution to (2.2) and (2.3)-(2.4) such that*

$$\mathcal{U}^\varepsilon(t = 0) = \mathcal{V}^\varepsilon(t = 0) = \varepsilon^\alpha(e^{i\theta}u_0 + c.c.).$$

Moreover

$$\frac{1}{\varepsilon^\alpha}\left|\Pi_1(kD_\theta + \varepsilon D_X)(\mathcal{U}^\varepsilon - \mathcal{V}^\varepsilon)\right|_{X_T} = O(\varepsilon^{2\alpha(q-1)+1})$$

and

$$\frac{1}{\varepsilon^\alpha}\left|\Pi_j(kD_\theta + \varepsilon D_X)\mathcal{U}^\varepsilon\right|_{X_T} = O(\varepsilon^{\alpha(q-1)+1}) \text{ for } j \geq 2.$$

Remark 2.1 *The scalling* ε^α *allows us to see how the error estimate evolves when the nonlinear effects decrease. Indeed, for large* α*, the nonlinear estimate is better than for small* α*. The case* $\alpha = \infty$ *correspond to the linear regime and the solution is then exact.*

Remark 2.2 *As usual for the proofs using WKB-type method, we need a lot of regularity on the approximate solution* $\mathcal{V}^\varepsilon$*. Therefore, we will impose the initial data* u_0 *to be more regular than the space in wich we want the error estimates [14].*

Now, we can introduce a second model as follows. Thanks to hypothesis 5, we expect the Fourier coefficients of order different from ± 1 of $\mathcal{V}^\varepsilon$ to be small. We therefore expect $\mathcal{V}^\varepsilon \approx \mathcal{V}_1^\varepsilon(t,X)e^{i\theta} + c.c.$. We therefore introduce the function $H^\varepsilon(t,X)$ solution to

$$\begin{aligned}\left(\partial_t + \frac{1}{\varepsilon}\left(-i\omega + i\lambda_1(k+\varepsilon D_X)\right)\right)\Pi_1(k+\varepsilon D_X)H^\varepsilon \\ = \Pi_1(k+\varepsilon D_X)C_1\left(f(H^\varepsilon e^{i\theta} + c.c.)\right)\end{aligned} \tag{2.5}$$

and we expect $H^\varepsilon e^{i\theta} + c.c.$ to be a good approximation of $\mathcal{V}^\varepsilon$ and hence of $\mathcal{U}^\varepsilon$. Our second result reads as follows.

Theorem 2.2 *Under the same hypothesis than for theorem 2.1. There exists T_0 independent of ε such that $T \geq T_0 > 0$ and a unique solution $H^\varepsilon(t,X) \in L^\infty(0,T_0;H^s_X(\mathbb{R}^n))$ to (2.5) satisfying $H^\varepsilon(0,X) = \varepsilon^\alpha u_0(x)$ and moreover*

$$\frac{1}{\varepsilon^\alpha}\left|C_1\left(\mathcal{V}^\varepsilon\right) - H^\varepsilon(t,X)\right|_{L^\infty(0,T_0;H^s_X(\mathbb{R}^n))} = O(\varepsilon^{2\alpha(q-1)+1})$$

and

$$\frac{1}{\varepsilon^\alpha}\left|\mathcal{V}^\varepsilon - \left(H^\varepsilon e^{i\theta} + c.c.\right)\right|_{X_T} = O(\varepsilon^{\alpha(q-1)+1}).$$

Remark 2.3 • *The error estimate between $\mathcal{V}^\varepsilon$ and $H^\varepsilon e^{i\theta} + c.c.$ is of the same type than that between $\mathcal{V}^\varepsilon$ and $\mathcal{U}^\varepsilon$.*
• *The equation satisfied by H^ε is not stiff anymore since $\lambda_1(k) = \omega$.*

2.2 Proofs of the theorems

We begin by the proof of theorem 2.1. One first has an obvious existence result for (2.2) and (2.3).

Proposition 2.1 *Let $u_0(X) \in H^\sigma(\mathbb{R}^n)$ (for σ large enough) and $s > \dfrac{n+1}{2}$. There exists $T > 0$ (independent of ε) such that there exists a unique solution $\mathcal{U}^\varepsilon$ to (2.2) and there exists a unique solution $\mathcal{V}^\varepsilon$ to (2.3) satisfying*

$$\mathcal{U}^\varepsilon \in \mathcal{C}([0,T];H^s(\mathbb{R}^n_X \times \mathbb{T}_\theta)), \quad \mathcal{V}^\varepsilon \in \mathcal{C}([0,T];H^s(\mathbb{R}^n_X \times \mathbb{T}_\theta))$$

and

$$\mathcal{U}^\varepsilon(t=0,\theta,X) = \mathcal{V}^\varepsilon(t=0,\theta,X) = \varepsilon^\alpha(e^{i\theta}u_0(X) + c.c.).$$

Moreover, there exists C independent of ε such that

$$\frac{1}{\varepsilon^\alpha}\left|\mathcal{U}^\varepsilon\right|_{X_T} + \frac{1}{\varepsilon^\alpha}\left|\mathcal{V}^\varepsilon\right|_{X_T} \leq C.$$

This proposition is obtained by usual energy estimates. It is of course not sufficient in order to prove theorem 2.1. Let us introduce

$$\mathcal{W}^\varepsilon = \frac{1}{\varepsilon^\alpha}\left(\mathcal{U}^\varepsilon - \mathcal{V}^\varepsilon\right) \tag{2.6}$$

and we consider the following decomposition of $\mathcal{W}^\varepsilon$:

$$\begin{aligned}\mathcal{W}^\varepsilon &:= \Pi_1(kD_\theta + \varepsilon D_X)\mathcal{W}^\varepsilon + \sum_{j=2}^{m} \Pi_j(kD_\theta + \varepsilon D_X)\mathcal{W}^\varepsilon, \\ &:= \varepsilon^{2\alpha(q-1)+1} a + \sum_{j=2}^{m} \varepsilon^{\alpha(q-1)+1} b_j.\end{aligned} \tag{2.7}$$

In order to prove theorem 2.1, it is enough to show that the functions a and b_j are bounded in $X_T = L^\infty([0,T]; H^s(\mathbb{R}^n_X \times \mathbb{T}_\theta))$. Let us now write the equations satisfied respectively by a and b_j. Let us form the difference of (2.3) from (2.2) and then apply the projector Π_j. Decomposition (2.1) yields (using the fact that f is an homogeneous polynomial of degree q)

$$\begin{aligned}\left(\partial_t + \frac{1}{\varepsilon}\left(-i\omega D_\theta + i\lambda_1(kD_\theta + \varepsilon D_X)\right)\right) a = \frac{1}{\varepsilon^{\alpha(q-1)+1}} \Pi_1(kD_\theta + \varepsilon D_X) \cdot \\ \cdot \left[f\left(\varepsilon^{2\alpha(q-1)+1} a + \sum_{j=2}^{m} \varepsilon^{\alpha(q-1)+1} b_j + \frac{1}{\varepsilon^\alpha}\mathcal{V}^\varepsilon\right) - f\left(\frac{1}{\varepsilon^\alpha}\mathcal{V}^\varepsilon\right)\right],\end{aligned} \tag{2.8}$$

and

$$\begin{aligned}&\left(\partial_t + \frac{1}{\varepsilon}\left(-i\omega D_\theta + i\lambda_j(kD_\theta + \varepsilon D_X)\right)\right) b_j \\ &= \frac{1}{\varepsilon}\Pi_j(kD_\theta + \varepsilon D_X)\left[f\left(\varepsilon^{2\alpha(q-1)+1} a + \sum_{j=2}^{m} \varepsilon^{\alpha(q-1)+1} b_j + \frac{1}{\varepsilon^\alpha}\mathcal{V}^\varepsilon\right)\right],\end{aligned} \tag{2.9}$$

for $j = 2$ to m. We start with equation (2.8). We first use Taylor's formula in the right-hand side of (2.8):

$$\begin{aligned}&f\left(\varepsilon^{2\alpha(q-1)+1} a + \sum_{j=2}^{m} \varepsilon^{\alpha(q-1)+1} b_j + \frac{1}{\varepsilon^\alpha}\mathcal{V}^\varepsilon\right) - f\left(\frac{1}{\varepsilon^\alpha}\mathcal{V}^\varepsilon\right) = \\ &= \int_0^1 f'\left(\frac{1}{\varepsilon^\alpha}\mathcal{V}^\varepsilon + \nu\left(\varepsilon^{2\alpha(q-1)+1} a + \sum_{j=2}^{m} \varepsilon^{\alpha(q-1)+1} b_j\right)\right) \cdot \\ &\cdot \left(\varepsilon^{2\alpha(q-1)+1} a + \sum_{j=2}^{m} \varepsilon^{\alpha(q-1)+1} b_j\right) d\nu.\end{aligned}$$

f is an homogeneous polynomial of degree q since H^s is an algebra for s large enough, hence this quantity can be estimated in $H^s_{\theta,X}$ norm by:

$$\Delta_1(t) = \left| f(\left(\varepsilon^{2\alpha(q-1)+1} a + \sum_{j=2}^{m} \varepsilon^{\alpha(q-1)+1} b_j + \frac{1}{\varepsilon^\alpha} \mathcal{V}^\varepsilon \right) - f\left(\frac{1}{\varepsilon^\alpha} \mathcal{V}^\varepsilon \right) \right|_{H^s},$$

$$\leq C\varepsilon^{\alpha(q-1)+1} \left(|\frac{\mathcal{V}^\varepsilon}{\varepsilon^\alpha}|^{q-1}_{H^s} + |a|^{q-1}_{H^s} + \sum_{j=2}^{m} |b_j|^{q-1}_{H^s} \right) \cdot \left(|a|_{H^s} + \sum_{j=2}^{m} |b_j|_{H^s} \right). \quad (2.10)$$

We now use an integral formulation of (2.8):

$$a = e^{-\frac{1}{\varepsilon}(-i\omega D_\theta + i\lambda_1(kD_\theta + \varepsilon D_X))t} a(t=0)$$

$$+ \int_0^t \frac{1}{\varepsilon^{\alpha(q-1)+1}} e^{-\frac{1}{\varepsilon}(-i\omega D_\theta + i\lambda_1(kD_\theta + \varepsilon D_X))(t-\tau)} \Pi_1(kD_\theta + \varepsilon D_X) \cdot$$

$$\cdot \left[f\left(\varepsilon^{2\alpha(q-1)+1} a(\tau) + \sum_{j=2}^{m} \varepsilon^{\alpha(q-1)+1} b_j(\tau) + \frac{1}{\varepsilon^\alpha} \mathcal{V}^\varepsilon(\tau) \right) - f\left(\frac{1}{\varepsilon^\alpha} \mathcal{V}^\varepsilon(\tau) \right) \right] d\tau$$

and using (2.10)

$$|a|_{H^s}(t) \leq |a(0)|_{H^s} + C \int_0^t \left(|\frac{\mathcal{V}^\varepsilon}{\varepsilon^\alpha}|^{q-1}_{H^s} + |a|^{q-1}_{H^s} + \sum_{j=2}^{m} |b_j|^{q-1}_{H^s} \right) \cdot \left(|a|_{H^s} + \sum_{j=2}^{m} |b_j|_{H^s} \right) d\tau.$$

Using the fact that $\frac{1}{\varepsilon^\alpha} |\mathcal{V}^\varepsilon|_{H^s}$ is bounded thanks to proposition 2.1 and that $a(t=0) = 0$, one gets

$$|a|_{H^s}(t) \leq C \int_0^t \left(1 + |a|_{H^s} + \sum_{j=2}^{m} |b_j|_{H^s} \right)^q (\tau) d\tau. \quad (2.11)$$

We now deal with equation (2.9). The main point is to recover one power of ε with respect to the right hand side using the "elliptic inversion" corresponding to the operator $-i\omega D_\theta + i\lambda_j(kD_\theta + \varepsilon D_X)$. We first rewrite equation (2.9) as follows:

$$\left(\partial_t + \frac{1}{\varepsilon} \left(-i\omega D_\theta + i\lambda_j(kD_\theta + \varepsilon D_X) \right) \right) b_j$$

$$= \frac{1}{\varepsilon} \Pi_j(kD_\theta + \varepsilon D_X) \left[f\left(\varepsilon^{2\alpha(q-1)+1} a + \sum_{j=2}^{m} \varepsilon^{\alpha(q-1)+1} b_j + \frac{1}{\varepsilon^\alpha} \mathcal{V}^\varepsilon \right) \right], \quad (2.12)$$

we write the nonlinear term under the form

$$f\left(\varepsilon^{2\alpha(q-1)+1}a+\sum_{j=2}^{m}\varepsilon^{\alpha(q-1)+1}b_j+\frac{1}{\varepsilon^\alpha}\mathcal{V}^\varepsilon\right)-f\left(\frac{\mathcal{V}^\varepsilon}{\varepsilon^\alpha}\right)+f\left(\frac{\mathcal{V}^\varepsilon}{\varepsilon^\alpha}\right).$$

An integral formula for (2.12) gives:

$$\begin{aligned}
b_j &= \frac{1}{\varepsilon}\int_0^t e^{-\frac{1}{\varepsilon}(-i\omega D_\theta+i\lambda_j(kD_\theta+\varepsilon D_X))(t-\tau)}\Pi_j(kD_\theta+\varepsilon D_X)\\
&\cdot\left[f\left(\varepsilon^{2\alpha(q-1)+1}a+\sum_{j=2}^{m}\varepsilon^{\alpha(q-1)+1}b_j+\frac{\mathcal{V}^\varepsilon}{\varepsilon^\alpha}\right)-f\left(\frac{\mathcal{V}^\varepsilon}{\varepsilon^\alpha}\right)\right](\tau)d\tau\\
&+\frac{1}{\varepsilon}\int_0^t e^{-\frac{1}{\varepsilon}(-i\omega D_\theta+i\lambda_j(kD_\theta+\varepsilon D_X))(t-\tau)}\Pi_j(kD_\theta+\varepsilon D_X)f\left(\frac{\mathcal{V}^\varepsilon}{\varepsilon^\alpha}\right)(\tau)d\tau,\\
&:= c_j+d_j.
\end{aligned}\tag{2.13}$$

Obviously, one has in the same way that for the estimate of a:

$$|c_j|_{H^s}(t)\leq C\int_0^t\left(1+|a|_{H^s}+\sum_{j=2}^{m}|b_j|_{H^s}\right)^q(\tau)d\tau.\tag{2.14}$$

We still have to estimate the term d_j. The idea is to perform the elliptic inversion on the nonlinear term associated with $\mathcal{V}^\varepsilon$ (that is $f(\mathcal{V}^\varepsilon)$ which is relatively well-known (at least asymptotically)). We introduce $\beta_j(D)=-\omega D_\theta+\lambda_j(kD_\theta+\varepsilon D_X)$ and the term d_j can be therefore written:

$$d_j=\frac{1}{\varepsilon}\int_0^t\Pi_j(kD_\theta+\varepsilon D_X)e^{-\frac{i}{\varepsilon}\beta_j(D)(t-\tau)}f\left(\frac{\mathcal{V}^\varepsilon}{\varepsilon^\alpha}\right)(\tau)d\tau.\tag{2.15}$$

In order to use the oscillatory behavior of the exponential, we split the function $\mathcal{V}^\varepsilon$ into a low-frequency and a high-frequency part

$$\begin{aligned}
\mathcal{V}^\varepsilon &= \mathbf{1}_{\left\{|D_X|\leq\frac{1}{\sqrt{\varepsilon}}\right\}}\mathcal{V}^\varepsilon+\mathbf{1}_{\left\{|D_X|>\frac{1}{\sqrt{\varepsilon}}\right\}}\mathcal{V}^\varepsilon,\\
&:= \mathcal{V}_1^\varepsilon+\mathcal{V}_2^\varepsilon.
\end{aligned}$$

Again, we write d_j as follows:

$$\begin{aligned}
d_j &= \frac{1}{\varepsilon}\int_0^t\Pi_j(kD_\theta+\varepsilon D_X)e^{-\frac{i}{\varepsilon}\beta_j(D)(t-\tau)}\left[f\left(\frac{\mathcal{V}^\varepsilon(\tau)}{\varepsilon^\alpha}\right)-f\left(\frac{\mathcal{V}_1^\varepsilon(\tau)}{\varepsilon^\alpha}\right)\right]d\tau,\\
&+\frac{1}{\varepsilon}\int_0^t\Pi_j(kD_\theta+\varepsilon D_X)e^{-\frac{i}{\varepsilon}\beta_j(D)(t-\tau)}f\left(\frac{\mathcal{V}_1^\varepsilon(\tau)}{\varepsilon^\alpha}\right)d\tau,\\
&:= e_j+f_j.
\end{aligned}\tag{2.16}$$

We begin by estimating e_j

$$e_j = \frac{1}{\varepsilon}\int_0^t \Pi_j(kD_\theta + \varepsilon D_X)e^{-\frac{i}{\varepsilon}\beta_j(D)(t-\tau)}\int_0^1 f'\left(\frac{\mathcal{V}_1^\varepsilon + \alpha\mathcal{V}_2^\varepsilon}{\varepsilon^\alpha}\right)\cdot\frac{\mathcal{V}_2^\varepsilon}{\varepsilon^\alpha}d\alpha d\tau,$$

and

$$|e_j|_{H^s} \leq \frac{1}{\varepsilon}\int_0^t\left(\left|\frac{\mathcal{V}_1^\varepsilon}{\varepsilon^\alpha}\right|_{H^s}^{q-1} + \left|\frac{\mathcal{V}_2^\varepsilon}{\varepsilon^\alpha}\right|_{H^s}^{q-1}\right)\frac{|\mathcal{V}_2^\varepsilon|_{H^s}}{\varepsilon^\alpha}d\tau.$$

Now since

$$\frac{|\mathcal{V}_i^\varepsilon|_{H^s}}{\varepsilon^\alpha} \leq \frac{|\mathcal{V}^\varepsilon|_{H^s}}{\varepsilon^\alpha}$$

for $i = 1, 2$ and thanks to proposition 2.1, $\dfrac{|\mathcal{V}^\varepsilon|_{H^s}}{\varepsilon^\alpha}$ is bounded, one has

$$\left|\frac{\mathcal{V}_1^\varepsilon}{\varepsilon^\alpha}\right|_{H^s}^{q-1} + \left|\frac{\mathcal{V}_2^\varepsilon}{\varepsilon^\alpha}\right|_{H^s}^{q-1} \leq C,$$

one gets:

$$|e_j|_{H^s} \leq \frac{C}{\varepsilon}\int_0^t \frac{|\mathcal{V}_2^\varepsilon(\tau)|_{H^s}}{\varepsilon^\alpha}d\tau.$$

Moreover, for all $N \in \mathbb{N}$ and for all $s \in \mathbb{R}$

$$\left|\mathcal{V}^\varepsilon \mathbf{1}_{\left\{|D_X|>\frac{1}{\sqrt{\varepsilon}}\right\}}\right|_{H^s} \leq C\varepsilon^N |\mathcal{V}^\varepsilon|_{H^{s+2N}}$$

and therefore

$$|e_j|_{H^s}(t) \leq Ct. \tag{2.17}$$

We now deal with the term f_j

$$f_j = \frac{1}{\varepsilon}\int_0^t \Pi_j(kD_\theta + \varepsilon D_X)e^{-\frac{i}{\varepsilon}\beta_j(D)(t-\sigma)}f\left(\frac{\mathcal{V}_1^\varepsilon(\sigma)}{\varepsilon^\alpha}\right).$$

Now thanks to hypothesis 4, one can apply the following result of nonlinear geometrical optics (see [14]): there exists a regular function $F(t, X)$ (independent of ε) such that

$$\frac{\mathcal{V}^\varepsilon}{\varepsilon^\alpha} = F(t, X)e^{i\theta} + c.c. + O(\varepsilon),$$

the $O(\varepsilon)$ being for example in $L^\infty(0, T; H^s_{\theta,X}(\mathbb{R}^n \times \mathbb{T}))$ norm. Plugging this expression into the expression of f_j yields

$$f_j = \frac{1}{\varepsilon}\int_0^t \Pi_j(kD_\theta + \varepsilon D_X)e^{-\frac{i}{\varepsilon}\beta_j(D)(t-\sigma)}f\left(\mathbf{1}_{\left\{|D_X|\leq\frac{1}{\sqrt{\varepsilon}}\right\}}\left(F(t, X)e^{i\theta} + c.c.\right)\right)d\sigma$$

$$+tO(1) := h_j + O(t).$$

Now, since f is an homogeneous polynomial of degree q,

$$f\left(\mathbf{1}_{\left\{|D_X|\leq\frac{1}{\sqrt{\varepsilon}}\right\}}\left(F(t, X)e^{i\theta} + c.c.\right)\right)$$

has the form:

$$f\left(\mathbf{1}_{\left\{|D_X|\leq\frac{1}{\sqrt{\varepsilon}}\right\}}\left(F(t,X)e^{i\theta}+c.c.\right)\right)=\sum_{\beta=-q}^{q}a_\beta^\varepsilon(t,X)e^{i\beta\theta},$$

where $a_\beta^\varepsilon(t,X)$ are regular functions, bounded independently of ε in spaces like $W^{k,\infty}(0,T;H_X^s(\mathbb{R}^n))$ for k large enough. Moreover, since the a_β^ε are products of components of $\mathbf{1}_{\left\{|D_X|\leq\frac{1}{\sqrt{\varepsilon}}\right\}}F$ and $\mathbf{1}_{\left\{|D_X|\leq\frac{1}{\sqrt{\varepsilon}}\right\}}\bar{F}$, the support of the Fourier transform of a_β^ε is included into $\left\{\xi/\quad|\xi|\leq\frac{q}{\sqrt{\varepsilon}}\right\}$. Taking the Fourier transform of h_j with respect to θ and X (denoting by $l\in\mathbb{Z}$ and $\xi\in\mathbb{R}^n$ the dual variables of θ and X) gives

$$\hat{h}_j(l,\xi,t)=\frac{1}{\varepsilon}\int_0^t\Pi_j(kl+\varepsilon\xi)e^{-\frac{i}{\varepsilon}[-l\omega+\lambda_j(kl+\varepsilon\xi)](t-\tau)}\hat{a}_l^\varepsilon(\tau,\xi)d\tau,\tag{2.18}$$

for $l=-q$ to q. Now thanks to hypothesis 5, for all l, $l\omega\neq\lambda_j(kl)$ since $j>1$. Moreover, since the support of $\xi\mapsto\hat{a}_l^\varepsilon(s,\xi)$ is included in $\left\{\xi/\quad|\xi|\leq\frac{q}{\sqrt{\varepsilon}}\right\}$, it follows that there exists $\varepsilon_0>0$ and $\delta>0$ such that $\forall\varepsilon\leq\varepsilon_0$, for all $l=-q$ to q, for all $\xi\in\left\{\xi/\quad|\xi|\leq\frac{q}{\sqrt{\varepsilon}}\right\}$,

$$|-l\omega+\lambda_j(kl+\varepsilon\xi)|\geq\delta.\tag{2.19}$$

We perform an integration by part in time on (2.18) and get:

$$\hat{h}_j(l,\xi,t)=\frac{1}{\varepsilon}\left[\frac{-i\varepsilon}{-l\omega+\lambda_j(kl+\varepsilon\xi)}e^{-\frac{i}{\varepsilon}[-l\omega+\lambda_j(kl+\varepsilon\xi)](t-\tau)}\Pi_j(kj+\varepsilon\xi)\hat{a}_l^\varepsilon(\tau,\xi)\right]_0^t$$

$$+\frac{1}{\varepsilon}\int_0^t\frac{i\varepsilon}{-l\omega+\lambda_j(kl+\varepsilon\xi)}e^{-\frac{i}{\varepsilon}[-l\omega+\lambda_j(kl+\varepsilon\xi)](t-\tau)}\Pi_j(kj+\varepsilon\xi)\partial_s\hat{a}_l^\varepsilon(\tau,\xi)d\tau.$$

Therefore using (2.19)

$$\left|\hat{h}_j(l,\xi,t)\right|\leq\frac{1}{\delta}\left(|\hat{a}_l^\varepsilon(t,\xi)|+|\hat{a}_l^\varepsilon(0,\xi)|\right)+\frac{1}{\delta}\int_0^t|\partial_\tau\hat{a}_l^\varepsilon(\tau,\xi)|d\tau$$

for all $l=-q$ to q. It follows that

$$|h_j|_{H^s}(t)\leq C(1+t)\tag{2.20}$$

One deduces that

$$|f_j|_{H^s}(t)\leq C(1+t)$$

and with (2.16) and (2.17) we get

$$|d_j|_{H^s}(t)\leq C(1+t).$$

Inequality (2.13) and estimate (2.14) give together with the above control of d_j:

$$|b_j|_{H^s} \leq C \int_0^t \left(1 + |a|_{H^s} + \sum_{j=2}^m |b_j|_{H^s}\right)^q (\tau) d\tau + C(1+t). \tag{2.21}$$

Now we recall the estimate (2.11) of a:

$$|a|_{H^s}(t) \leq C \int_0^t \left(1 + |a|_{H^s} + \sum_{j=2}^m |b_j|_{H^s}\right)^q (\tau) d\tau.$$

Introducing $y = 1 + |a|_{H^s} + \sum_{j=2}^m |b_j|_{H^s}$, one gets using (2.21)

$$y \leq c \int_0^t y^q(\sigma) d\sigma + C(1+t),$$

which implies that there exists $T_0 > 0$ and $C_0 > 0$ such that y is defined on $[0, T_0]$ and $|y|_{L^\infty(0,T_0)} \leq C_0$. This ends the proof of theorem 2.1.

2.3 Proof of theorem 2.2.

We will now compare the solution $\mathcal{V}^\varepsilon$ given by (2.3)-(2.4) and H^ε given by (2.5). The proof is mainly the same than for the previous result, we only sketch it. Introduce

$$\mathcal{V}^\varepsilon = \sum_{\beta \in \mathbb{Z}} \mathcal{V}^\varepsilon_\beta(t, X) e^{i\beta\theta}.$$

The equation satisfied by $\mathcal{V}^\varepsilon_\beta$ is

$$\left(\partial_t + \frac{1}{\varepsilon}\left(-i\omega\beta + i\lambda_1(k\beta + \varepsilon D_X)\right)\right) \Pi_1(k\beta + \varepsilon D_X) \mathcal{V}^\varepsilon_\beta = \Pi_1(k\beta + \varepsilon D_X) C_\beta\left(f(\mathcal{V}^\varepsilon)\right).$$

Introduce $X^\varepsilon = \frac{1}{\varepsilon^\alpha}\left[\mathcal{V}^\varepsilon_1 - H^\varepsilon\right]$ where H^ε is the solution to (2.5). The equation satisfied by $\frac{\mathcal{V}^\varepsilon_\beta}{\varepsilon^\alpha}$ for $\beta \neq 1$ or -1 is

$$\left(\partial_t + \frac{1}{\varepsilon}\left(-i\omega\beta + i\lambda_1(k\beta + \varepsilon D_X)\right)\right) \Pi_1(k\beta + \varepsilon D_X) \frac{\mathcal{V}^\varepsilon_\beta}{\varepsilon^\alpha} = \Pi_1(k\beta + \varepsilon D_X) \varepsilon^{\alpha(q-1)} C_\beta f(\frac{\mathcal{V}^\varepsilon_\beta}{\varepsilon^\alpha}).$$

An elliptic inversion on $\frac{\mathcal{V}^\varepsilon_\beta}{\varepsilon^\alpha}$ gives an estimate of $\frac{\mathcal{V}^\varepsilon_\beta}{\varepsilon^\alpha}$ of size $\varepsilon^{\alpha(q-1)+1}$ for $\beta \neq \pm 1$. Now the equation satisfied by X^ε is

$$\begin{aligned} &\left(\partial_t + \frac{1}{\varepsilon}\left(-i\omega + i\lambda_1(k + \varepsilon D_X)\right)\right) \Pi_1(k + \varepsilon D_X) X^\varepsilon \\ &= \Pi_1(k + \varepsilon D_X) \varepsilon^{\alpha(q-1)} \left[C_1\left(f(\frac{\mathcal{V}^\varepsilon_\beta}{\varepsilon^\alpha})\right) - C_1\left(f(\frac{H^\varepsilon e^{i\theta} + c.c.}{\varepsilon^\alpha})\right)\right]. \end{aligned} \tag{2.22}$$

Now write $\mathcal{V}^\varepsilon = \mathcal{V}_1^\varepsilon e^{i\theta} + c.c. + \tilde{\mathcal{V}}^\varepsilon$. Then the right-hand-side of (2.22) reads

$$C_1\left(f(\frac{\mathcal{V}_\beta^\varepsilon}{\varepsilon^\alpha})\right) - C_1\left(f(\frac{H^\varepsilon e^{i\theta}+c.c.}{\varepsilon^\alpha}\right)$$

$$= C_1\left(f\left(\frac{H^\varepsilon e^{i\theta}+c.c.}{\varepsilon^\alpha} + X^\varepsilon e^{i\theta} + c.c. + \frac{\tilde{\mathcal{V}}^\varepsilon}{\varepsilon^\alpha}\right) - f\left(\frac{H^\varepsilon e^{i\theta}+c.c.}{\varepsilon^\alpha}\right)\right),$$

$$\approx C_1\left(f'\left(\frac{H^\varepsilon e^{i\theta}+c.c.}{\varepsilon^\alpha}\right)\left[X^\varepsilon e^{i\theta} + c.c. + \frac{\tilde{\mathcal{V}}^\varepsilon}{\varepsilon^\alpha}\right]\right).$$

Integrating (2.22) in times gives

$$|X^\varepsilon|_{H^s}(t) \leq \int_0^t \varepsilon^{\alpha(q-1)} C|X^\varepsilon|_{H^s}(\sigma)d\sigma + \int_0^t C\varepsilon^{\alpha(q-1)}\left|\frac{\tilde{\mathcal{V}}^\varepsilon}{\varepsilon^\alpha}\right|_{H^s} d\sigma.$$

But $\dfrac{\tilde{\mathcal{V}}^\varepsilon}{\varepsilon^\alpha} = O(\varepsilon^{\alpha(q-1)+1})$. It follows that

$$|X|_{L^\infty(0,T;H^s)} = O(\varepsilon^{2\alpha(q-1)+1})$$

which is the desired result.

2.4 Some extensions.

Note that if $\alpha = 0$, that is for $O(1)$ solutions the error estimate is the same than for usual geometrical optics. The estimate is in fact better for $\alpha > 0$. Recall that ε^α is the size of the initial data and hence of the solution. But if $\alpha > 0$, then standard technics on (1.13) ensures existence for time of size $\dfrac{1}{\varepsilon^{\alpha(q-1)}}$. The natural question is then to know if our estimates are valid on such time interval. The answer is affirmative and one has

Theorem 2.3 *Under the same hypothesis than for theorem 2.1, there exists $T_1 > 0$ and $C_1 > 0$ (independent of ε) such that*

$$\frac{1}{\varepsilon^\alpha}\left|\Pi_1(kD_\theta + \varepsilon D_X)\left(\mathcal{U}^\varepsilon - \mathcal{V}^\varepsilon\right)\right|_{L^\infty(0,t;H^s_{\theta,X}(\mathbb{T}\times\mathbb{R}^n))} \leq C_1\varepsilon^{\alpha(q-1)+1}\left(e^{C_1\varepsilon^{\alpha(q-1)}t} - 1\right)$$

and

$$\frac{1}{\varepsilon^\alpha}\left|\Pi_1(kD_\theta + \varepsilon D_X)\mathcal{U}^\varepsilon\right|_{L^\infty(0,t;H^s_{\theta,X}(\mathbb{T}\times\mathbb{R}^n))} \leq C_1\varepsilon^{\alpha(q-1)+1}t,$$

as long as $t \leq \dfrac{T_1}{\varepsilon^{\alpha(q-1)}}$. Moreover

$$\frac{1}{\varepsilon^\alpha}\left|C_1\left(\mathcal{V}^\varepsilon(t,X,\theta)\right) - H^\varepsilon(t,X)\right|_{L^\infty(0,t;H^s_X(\mathbb{R}^n))} \leq C_1\varepsilon^{\alpha(q-1)+1}\left(e_1^{C_1\varepsilon^{\alpha(q-1)}} - 1\right)$$

and

$$\frac{1}{\varepsilon^\alpha}\left|\mathcal{V}^\varepsilon(t,X,\theta) - \left(H^\varepsilon(t,X)e^{i\theta} + c.c.\right)\right|_{L^\infty(0,t;H^s_{\theta,X}(\mathbb{T}\times\mathbb{R}^n))} \leq C_1\varepsilon^{\alpha(q-1)+1}t,$$

as long $t \leq \dfrac{T_1}{\varepsilon^{\alpha(q-1)}}$.

That means that our asymptotics are uniform on long time interval. See the next section for numerical illustrations of these results.

Remark 2.4 *Suppose that for all $X \in \mathbb{R}^n$, $f(X)\cdot X = 0$, then for any solution $\mathcal{V}^\varepsilon$ to (2.3) one has*

$$\int |\mathcal{V}^\varepsilon|^2(t)dXd\theta = \int |\mathcal{V}^\varepsilon|^2(0)dXd\theta$$

and for any solution H^ε to (2.5)

$$\int |H^\varepsilon|(t)dX = \int |H^\varepsilon|(0)dX.$$

That means that if the initial model is conservative, then the asymptotic one is conservative as well.

3 Some numerical results.

3.1 An example.

In this section, we want to compare numerically the solutions of the different asymptotic regimes and we want to see to which extent the error estimates that we have proved in the previous section are effective. We choose to make the computations on a simplified system which is dispersive, nonlinear and preserves the L^2 norm. This system is:

$$\begin{cases} \partial_t u + \partial_x v - \dfrac{v}{\varepsilon} = -(u^2+v^2)v, \\ \\ \partial_t v + \partial_x u + \dfrac{u}{\varepsilon} = (u^2+v^2)u. \end{cases} \tag{3.1}$$

The characteristic variety of this system is the set

$$\left\{(\omega,k) \in \mathbb{R}^2 / \quad \omega^2 = 1+k^2\right\}.$$

Hypothesis 3 and 4 are therefore satisfied. For hypothesis 5, suppose that $\omega^2 = 1+k^2$ and that for $m \in \mathbb{Z}$ one has $m^2\omega^2 = 1+m^2k^2$. It then follows that $m = \pm 1$ and hypothesis 5 is satisfied.
We now derive the asymptotic models corresponding to (3.1) in the geometrical and diffractive regimes. We refer for example to [13] for the case of diffractive optics.

3.1.1 The geometrical optics regime.

One search an approximate solution in the form:

$$\begin{pmatrix} u_0(t,x) \\ v_0(t,x) \end{pmatrix} e^{i\frac{kx-\omega t}{\varepsilon}} + c.c..$$

Then one obtains

$$u_0 = \frac{ik-1}{i\omega} v_0 \tag{3.2}$$

and

$$\partial_t u_0 + \frac{k}{\omega}\partial_x u_0 = \frac{4i}{\omega}|u_0|^2 u_0, \text{ for } t \in [0, T_0]. \tag{3.3}$$

3.1.2 Diffractive optics.

One search an approximate solution in the form

$$\begin{pmatrix} u_1(t,x) \\ v_1(t,x) \end{pmatrix} e^{i\frac{kx-\omega t}{\varepsilon}} + c.c.,$$

but on long time-scale with $u_1(0,x) = O(\sqrt{\varepsilon})$, $v_1(0,x) = O(\sqrt{\varepsilon})$. One gets

$$u_1 = \frac{ik-1}{i\omega} v_1 \tag{3.4}$$

and

$$\partial_t u_1 + \frac{k}{\omega}\partial_x u_1 - \frac{i\varepsilon}{\omega^3}\partial_x^2 u_1 = \frac{4i}{\omega}|u_1|^2 u_1, \text{ for } t \in [0, \frac{T_1}{\varepsilon}]. \tag{3.5}$$

3.1.3 The new model.

One search for a solution in the form

$$\begin{pmatrix} u_2(t,x) \\ v_2(t,x) \end{pmatrix} e^{i\frac{kx-\omega t}{\varepsilon}} + c.c.$$

and one gets

$$u_2 = \frac{i(k+\varepsilon D_x)-1}{i\sqrt{1+(k+\varepsilon D_x)^2}} v_2 \tag{3.6}$$

and

$$\partial_t \begin{pmatrix} u_2 \\ v_2 \end{pmatrix} + \frac{i}{\varepsilon}\left(\sqrt{1+(k+\varepsilon D_x)^2} - \sqrt{1+k^2}\right)\begin{pmatrix} u_2 \\ v_2 \end{pmatrix}$$

$$= \begin{pmatrix} \frac{1}{2} & \frac{i(k+\varepsilon D_x)-1}{2i\sqrt{1+(k+\varepsilon D_x)^2}} \\ \frac{i(k+\varepsilon D_x)+1}{2i\sqrt{1+(k+\varepsilon D_x)^2}} & \frac{1}{2} \end{pmatrix} \begin{pmatrix} -2(|u_2|^2+|v_2|^2)v_2 - (u_2^2+v_2^2)\bar{v}_2 \\ -2(|u_2|^2+|v_2|^2)u_2 - (u_2^2+v_2^2)\bar{u}_2 \end{pmatrix}. \tag{3.7}$$

Of course thanks to (3.6), we can restrict ourselves to the first equation of (3.7) and setting

$$\mu^\varepsilon(D_x) = \frac{i(k+\varepsilon D_x) - 1}{i\sqrt{1+(k+\varepsilon D_x)^2}},$$

one obtains

$$\begin{aligned} &\partial_t u_2 + \frac{k\partial_x - i\varepsilon\partial_x^2}{\sqrt{1+(k+\varepsilon D_x)^2}+\sqrt{1+k^2}}u_2 \\ &= -(|u_2|^2+|v_2|^2)v_2 - 2(u_2^2+v_2^2)\bar{v}_2 \\ &+\mu^\varepsilon(D_x)\left[(|u_2|^2+|v_2|^2)u_2 + 2(u_2^2+v_2^2)\bar{u}_2\right] \end{aligned} \tag{3.8}$$

with

$$v_2 = \frac{1}{\mu^\varepsilon(D_x)}u_2, \tag{3.9}$$

which is the complete system.
Finally, the same system with the Kerr nonlinearity is used in practical applications in [17] and reads

$$\partial_t u_3 + \frac{k\partial_x - i\varepsilon\partial_x^2}{\sqrt{1+(k+\varepsilon D_x)^2}+\sqrt{1+k^2}}u_3 = \frac{4i}{\omega}|u_3|^2u_3. \tag{3.10}$$

We will also compare our system with that one.

3.2 The numerical method.

We restrict ourself to the case $x \in [0,1]$ with periodic boundary conditions and we use a spectral method in the space variable x. For time discretization, we adopt a splitting technique.
• For system (3.1), suppose we have built an approximate solution $(u(n\delta t), v(n\delta t))$ at time $n\delta t$; one first integrates the linear part explicitly in Fourier variables with initial data $(u(n\delta t), v(n\delta t))$ over one time step. This gives an indermediate value (u_i, v_i). Then one integrates the nonlinear part

$$\partial_t \begin{pmatrix} u \\ v \end{pmatrix} = \begin{pmatrix} -(|u|^2+|v|^2)v \\ (|u|^2+|v|^2)u \end{pmatrix}$$

with initial value (u_i, v_i) explicitly over one time step. This gives $(u((n+1)\delta t), v((n+1)\delta t)$.
• For the geometrical optics equation (3.3) one has the exact solution

$$u_0(t,x) = A(x - \frac{k}{\omega}t)e^{\frac{4i}{\omega}|A(x-\frac{k}{\omega}t)|^2 t}, \tag{3.11}$$

where $A(x) = u_0(0,x)$.
• For the diffractive regime (3.5) we use the same strategy than for (3.1). We omit the details since it is a standard procedure for the nonlinear Schrödinger

equation (see [4] and reference therein for a more detailed study).
For the new model (3.8). Suppose that one has the Fourier transform of $u_2(n\delta t)$: $\hat{u}_2(n\delta t)$. One solves the linear part of (3.8):

$$\partial_t \hat{u}_2 + \frac{ik\xi + \varepsilon\xi^2}{\sqrt{1+(k+\varepsilon\xi)^2} + \sqrt{1+k^2}}\hat{u}_2 = 0,$$

with initial value $\hat{u}_2(n\delta t, \xi)$ on one time step. One gets an intermediate value $\hat{u}_{2i}$. One then obtains an intermediate value of $\hat{v}_2$ called $\hat{v}_{2i}$ using (3.9). We then perform an inverse Fourier transform of $\hat{u}_{2i}$ and $\hat{v}_{2i}$ in order to obtain u_{2i} and v_{2i} and then one construct the nonlinear terms

$$NL1 := -(|u_{2i}|^2 + |v_{2i}|^2)v_{2i} - 2(u_{2i}^2 + v_{2i}^2)\bar{v}_{2i}$$

and

$$NL2 := (|u_{2i}|^2 + |v_{2i}|^2)u_{2i} + 2(u_{2i}^2 + v_{2i}^2)\bar{u}_{2i}.$$

Next we perform a Fourier transform of $NL1$ and $NL2$ and compute $\hat{N}L1 + \mu^\varepsilon(\xi)\hat{N}L2$. The value of $\hat{u}_2((n+1)\delta t)$ is obtained by the explicit Euler scheme

$$\hat{u}_2((n+1)\delta t) = \hat{u}_{2i} + \delta t\left[\hat{N}L1 + \mu^\varepsilon(\xi)\hat{N}L2\right].$$

• For the modified system (3.10) the nonlinear step is explicit just like for (3.5) or (3.1).

All these schemes are of order 1 in time.

3.3 Numerical results.

We have performed simulations with $\varepsilon = 10^{-2}$ or $\varepsilon = 10^{-3}$. All the results are given in the case where the numerical solution has converged, that is a division of the time step by 2 and a multiplication by 2 of the number of points for the spatial discretization does not change the result. We use L^2 norms in order to compare the solutions. We take an initial value for u in the form

$$u(t=0,x) = \varepsilon^\alpha\left(e^{i\frac{kx}{\varepsilon}}\varphi(x) + c.c.\right),$$

for $\alpha \geq 0$. All the simulations are done with $k = 2\pi$ and $\omega = \sqrt{1+(2\pi)^2}$. The initial value for v is obtained by using (3.9). That means that one takes: $\psi(x) = \dfrac{1}{\mu^\varepsilon(D_x)}\varphi(x)$ and

$$v(t=0,x) = \varepsilon^\alpha\left(e^{i\frac{kx}{\varepsilon}}\psi(x) + c.c.\right).$$

The initial data for u_0, u_1, u_2 and u_3 is of course $\varphi(x)$. We call

$$e_{geo} = \max_{t\in[0,T]} \frac{\left|u(t,\cdot) - \varepsilon^\alpha(u_0(t,\cdot)e^{i\frac{kx-\omega t}{\varepsilon}} + c.c.)\right|_2}{|u(t,\cdot)|_2},$$

that is the maximum of the error between the exact solution of (3.1) and the approximate solution given by the geometrical optics approximation (3.3) on the time intervale $[0,T]$. Here $|f|_2$ denotes the L^2 norm on $[0,1]$ of the function f. We also introduce

$$e_{diff} = \max_{t\in[0,T]} \frac{\left|u(t,\cdot) - \varepsilon^\alpha (u_1(t,\cdot)e^{i\frac{kx-\omega t}{\varepsilon}} + c.c.)\right|_2}{|u(t,\cdot)|_2},$$

that is the maximum of the error between the exact solution of (3.1) and the approximate solution given by the diffractive optics approximation (3.5) on the time intervale $[0,T]$ and

$$e_{new} = \max_{t\in[0,T]} \frac{\left|u(t,\cdot) - \varepsilon^\alpha (u_2(t,\cdot)e^{i\frac{kx-\omega t}{\varepsilon}} + c.c.)\right|_2}{|u(t,\cdot)|_2},$$

that is the maximum of the error between the exact solution of (3.1) and the approximate solution given by the new model on the time intervale $[0,T]$ and

$$e_{newkerr} = \max_{t\in[0,T]} \frac{\left|u(t,\cdot) - \varepsilon^\alpha (u_3(t,\cdot)e^{i\frac{kx-\omega t}{\varepsilon}} + c.c.)\right|_2}{|u(t,\cdot)|_2},$$

that is the maximum of th error between the exact solution of (3.1) and the approximate solution given by the new model with Kerr nonlinearity given by (3.10) on the time intervale $[0,T]$. We denote by N the number of Fourier modes in space and N_t the number of time steps.

3.3.1 Time of order 1.

• Case 1. We begin with $\varphi(x) = e^{-75(x-\frac{1}{2})^2} e^{i10\cos(x)}$ with $\alpha = 0$ and we compute for $x \in [0,1]$ and $t \in [0,1]$. The errors at $T = 1$ are:

	$\varepsilon = 10^{-2}$	$\varepsilon = 10^{-3}$
e_{geo}	$2\ 10^{-2}$	$2.3\ 10^{-3}$
e_{diff}	$2\ 10^{-2}$	$2.3\ 10^{-3}$
e_{new}	$1.9\ 10^{-2}$	$2\ 10^{-3}$
$e_{newkerr}$	$2\ 10^{-2}$	$2.3\ 10^{-3}$

For $\varepsilon = 10^{-2}$, the convergence on the errors is reached with $N = 1024$ and $N_t = 1600$. For $\varepsilon = 10^{-3}$ the convergence is reached with $N = 16384$ and $N_t = 12800$. For all cases, the error is of order ε as predicted by the theory. The simplest model (geometrical optics) is precise enough.
• Case 2. We made a test for smaller solutions, namelly $\alpha = \frac{1}{2}$. The error at $T = 1$ are

	$\varepsilon = 10^{-2}$	$\varepsilon = 10^{-3}$
e_{geo}	$3.3\ 10^{-3}$	$3.2\ 10^{-4}$
e_{diff}	$1.7\ 10^{-4}$	$1.8\ 10^{-6}$
e_{new}	$1.6\ 10^{-4}$	$1.9\ 10^{-6}$
e_{newker}	$1.9\ 10^{-4}$	$2\ 10^{-6}$

For $\varepsilon = 10^{-2}$, the convergence on the errors is reached with $N = 1024$ and $N_t = 1600$. For $\varepsilon = 10^{-3}$ the convergence is reached with $N = 16384$ and $N_t = 12800$. Basically, the error for geometrical optics is the worst (of order ε), however, it remains very satisfactory. The others are of order ε^2 as predicted by the theory.

• Case 3. For chirped initial data:

$$u(t = 0, x) = (e^{-75(x-1/2)^2} e^{i15cos(15x)} e^{i\frac{kx}{\varepsilon}} + c.c.),$$

$x \in [0, 1]$. Such kind of solution can occur after diffraction webs for example or for laser with large spectrum. The errors at $T = 1$ are:

	$\varepsilon = 10^{-2}$	$\varepsilon = 10^{-3}$
e_{geo}	0.8	$5.7\ 10^{-2}$
e_{diff}	0.17	$1.2\ 10^{-2}$
e_{new}	0.023	$1.9\ 10^{-3}$
$e_{newkerr}$	0.21	$1.4\ 10^{-2}$

For $\varepsilon = 10^{-2}$, the convergence on the errors is reached with $N = 1024$ and $N_t = 1600$. For $\varepsilon = 10^{-3}$ the convergence is reached with $N = 16384$ and $N_t = 12800$. For $\varepsilon = 10^{-2}$, the error for the complete new model is 2.3%, the other errors are above 15%. Such errors are not acceptable in practical applications. As an illustration, one can find on figure 5 the modulus of the amplitude (that is without the phase factor $e^{i\frac{(kx-\omega t)}{\varepsilon}}$) of the first component for the three models : the new model, the geometrical optics and the diffractive optics at the final time. As seen on the figure, the amplitude as well the positions are false for the diffractive and geometrical optics regimes.
For $\varepsilon = 10^{-3}$, the result given by Shrödinger equation and the new model with the Kerr nonlinearity are correct. The geometrical optics give the worst error and the complete new model the smallest one.

• Case 4. For smaller solutions: we made the same test but with $\alpha = \frac{1}{2}$. The errors are:

	$\varepsilon = 10^{-2}$	$\varepsilon = 10^{-3}$
e_{geo}	0.91	$6.9\ 10^{-2}$
e_{diff}	0.32	$2.3\ 10^{-3}$
e_{new}	$1.7\ 10^{-4}$	$1.7\ 10^{-6}$
$e_{newkerr}$	$2.1\ 10^{-3}$	$1.5\ 10^{-5}$

For $\varepsilon = 10^{-2}$, the convergence on the errors is reached with $N = 1024$ and $N_t = 1600$. For $\varepsilon = 10^{-3}$ the convergence is reached with $N = 16384$ and

$N_t = 12800$. As in the previous case, geometrical optics and the Schrödinger models give high errors for $\varepsilon = 0.01$. Both new models are correct however. For $\varepsilon = 10^{-3}$, the conclusions are the same than in the previous cases.

3.3.2 Diffractive time.

We now consider long time behavior : $T = 50$.
• Case 5. We begin by a regular initial data and we take $\varphi(x) = e^{-75(x-\frac{1}{2})^2} e^{i\cos(x)}$ and $\alpha = \dfrac{1}{2}$. One gets the following errors:

	$\varepsilon = 10^{-2}$	$\varepsilon = 10^{-3}$
e_{geo}	0.13	$1.3\ 10^{-2}$
e_{diff}	$2.4\ 10^{-3}$	$2\ 10^{-5}$
e_{new}	$1.7\ 10^{-4}$	$3\ 10^{-6}$
$e_{newkerr}$	$5.6\ 10^{-3}$	$5\ 10^{-5}$

For $\varepsilon = 10^{-2}$, the convergence on the errors is reached with $N = 2048$ and $N_t = 80000$. For $\varepsilon = 10^{-3}$ the convergence is reached with $N = 8192$ and $N_t = 320000$. The geometrical optics gives of course a false result since diffractive effects are important. The result given by the new models are better than that of diffractive optics that is however perfectly correct. Any of the three models can be used in practical applications.
• Case 6. For chirped initial data, we take

$$\varphi(x) = (e^{-75(x-1/2)^2} e^{i15cos(15x)} + c.c.),$$

$x \in [0, 1]$ and $\alpha = \dfrac{1}{2}$ for $T = 50$:

	$\varepsilon = 10^{-2}$	$\varepsilon = 10^{-3}$
e_{geo}	1.5	1.6
e_{diff}	1.4	0.11
e_{new}	$5\ 10^{-4}$	$3\ 10^{-6}$
$e_{newkerr}$	0.08	$8\ 10^{-4}$

For $\varepsilon = 10^{-2}$, the convergence on the errors is reached with $N = 2048$ and $N_t = 80000$. For $\varepsilon = 10^{-3}$ the convergence is reached with $N = 8192$ and $N_t = 320000$. Only the complete new model gives an acceptable error. All the others give bad result. The new model with Kerr nonlinearity gives a satisfactory result for small ε but not for $\varepsilon = 0.01$. One can see the evolution of the solution at time $n\dfrac{50}{8}$ on figure 3, and on figure 4 the same but with the solution given by the Schrödinger equation which is far away from the reality.

3.3.3 Conclusion

For small times, chirped initial data or not, the diffractive model is satisfactory. For diffractive times and not chirped initial data, the diffractive model is satisfactory. The geometrical optics regime (that is the explicit solution) is

valid on short times.
For diffractive times with chirped initial data, the new model is very useful. The new model with Kerr nonlinearity is intermediate in terms of quality. In any case the solution given by the new system can not be distinguish from the exact one and will be therefore very usefull in practical applications. We postpone the application of this theory to physical cases with more numerical test to further work.
The main problem of our theory is the boundary conditions. Clearly, because of the pseudo-differential nature of the new model, it is not easy to take into account non-periodic boundary conditions. One of the possibility in this direction is to take one space variable as variable of evolution. This process is under investigation.

References

[1] D. Alterman and J. Rauch, *Nonlinear geometric optics for short pulses*, J. Differential Equations 178 (2002), no. 2, 437–465.

[2] K. Barrailh and D. Lannes, *A general framework for diffractive optics and its applications to asers with large spectrum and short pulses*, to appear in SIAM Journ. for Math. Analysis 2003.

[3] J.-D. Benamou, O. Lafitte, R. Sentis and I. Solliec, *A geometric optics based numerical method for high frequency electromagnetic fields computations near fold caustics - Part I* , Preprint, INRIA tech. rep. RR-4422. (2002).

[4] C. Besse and B. Bidegaray, *Numerical study of self-focusing solutions to the schrödinger-debye system*, M2AN Math. Model. Numer. Anal. 1:35–55, 2001.

[5] B. Bidégaray, A. Bourgeade, D. Reignier and R. Ziolkowski, *Multi-level Maxwell-Bloch simulations*. In A. Bermúdez, D. Gómez, C. Hazard, P. Joly and J.E. Roberts, editors, *Mathematical and Numerical aspects of Wave Propagation*, pages 221-225, 2000.

[6] J. Bona, M. Chen and J.-C. Saut, *Boussinesq equations and other systems for small-amplitude long waves in nonlinear dispersive media. I. Derivation and linear theory*, J. Nonlinear Sci. 12 (2002), no. 4, 283–318.

[7] J. Bona, T. Colin, D. Lannes, *Long wave models for water-waves*, preprint Université Bordeaux 1, 2003.

[8] R.W. Boyd, *Nonlinear Optics*, Academic Press, 1992.

[9] T. Colin, *Rigorous derivation of the nonlinear Schrödinger equation and Davey-Stewartson systems from quadratic hyperbolic systems*, soumis à Asymptotic Analysis.

[10] T. Colin and B. Nkonga, *A numerical model for light interaction with a two-level atoms medium*, preprint Université Bordeaux 1, 2002.

[11] P. Donnat, *Quelques contributions mathématiques en optique non linéaire*, thèse Ecole Polytechnique 1994.

[12] P. Donnat, J.-L. Joly, G. Métivier and J. Rauch, *Diffractive nonlinear geometric optics,* Séminaire sur les équations aux Dérivées Partielles, 1995–1996, Exp. No. XVII. Ecole Polytech., Palaiseau, 1996.

[13] P. Donnat and J. rauch, *Dispersive nonlinear geometric optics*, J. Math. Phys., 38(1997),1484-1523.

[14] J.-L. Joly, G. Métivier and J. Rauch, *Generic rigorous asymptotic expansions for weakly nonlinear geometric optics*, Duke Math. J. 70, 373-404, 1993.

[15] J.-L. Joly, G. Métivier and J. Rauch, *Transparent nonlinear geometric optics and Maxwell-Bloch equations*, Journal of Differential Equations 166, 175-250, 2000.

[16] D. Lannes, *Dispersive effects for nonlinear geometrical optics with rectification*, Asymptotic Analysis 18, p.p. 111-146, 1998.

[17] O. Morice, *Reference Manual of code Miró*, CEA, France 2002.

[18] A. C. Newell and J. V. Moloney, *Nonlinear Optics*. Addison-Wesley Publiching Compagny, 1991.

[19] T. Schäfer and E. Wayne, *Propagation of ultra-short optical pulses in nonlinear media*, Preprint.

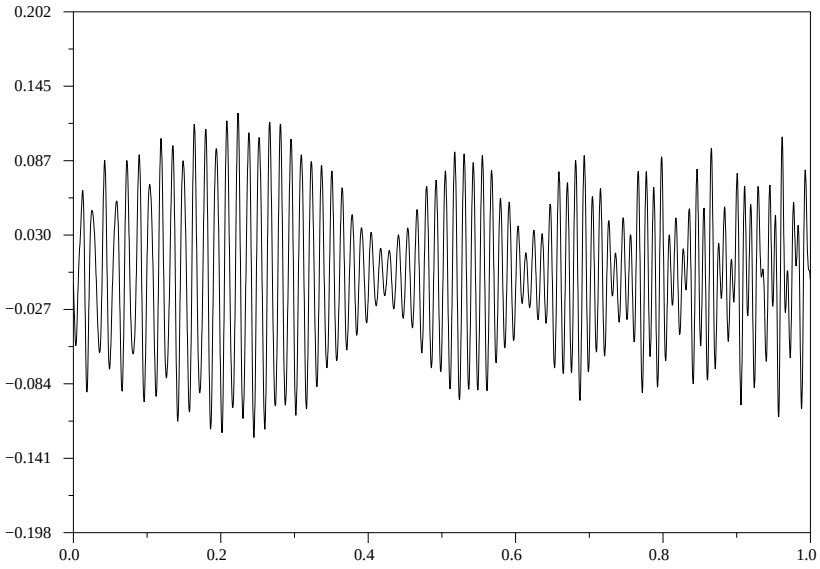

Figure 1: Real part of the first component of the solution of system (1.17) with $\varepsilon = 0.01$ at time $T = 50$, with chirped initial data, case 6.

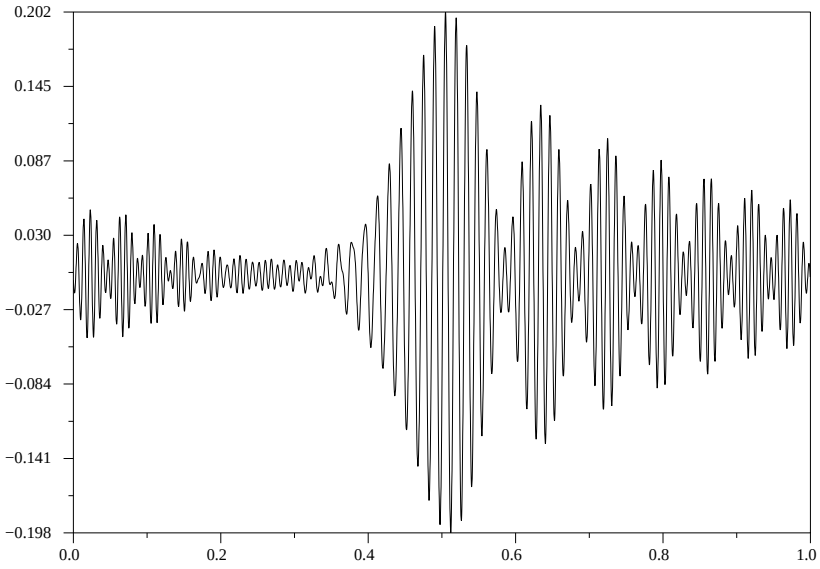

Figure 2: Real part of the approximate solution of the first component of system (1.17) with $\varepsilon = 0.01$ given by the nonlinear Schrödinger equation (3.5) at time $T = 50$, with chirped initial data, case 6

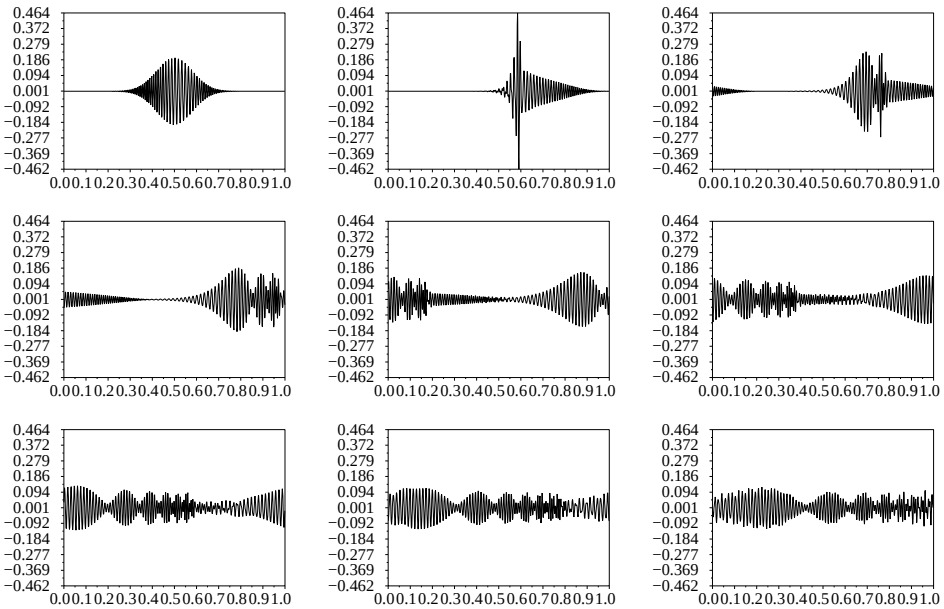

Figure 3: Real part of the first component of the solution of system (3.1) with $\varepsilon = 0.01$ at time $t = n\dfrac{50}{8}$ for $n = 0 \cdots 8$ with chirped initial data and $\alpha = 1/2$. First line, from left to right, $n = 0, 1, 2$, second line, from left to right, $n = 3, 4, 5$, third line, from left to right, $n = 6, 7, 8$, case 6.

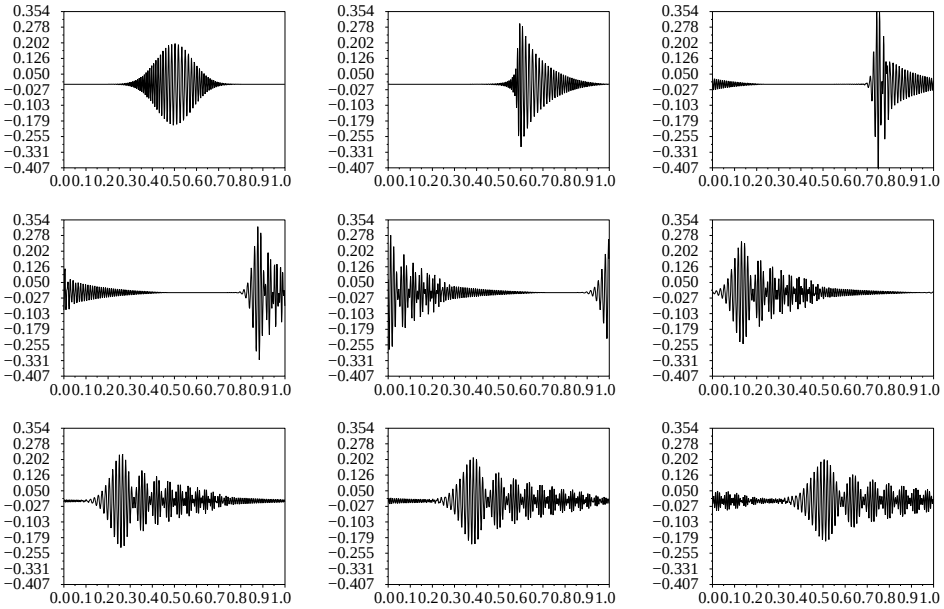

Figure 4: Real part of the approximate solution of system (3.1) with $\varepsilon = 0.01$ at time $t = n\dfrac{50}{8}$ for $n = 0 \cdots 8$ with chirped initial data and $\alpha = 1/2$ given by diffractive optics approximation. First line, from left to right, $n = 0, 1, 2$, second line, from left to right, $n = 3, 4, 5$, third line, from left to right, $n = 6, 7, 8$, case 6.

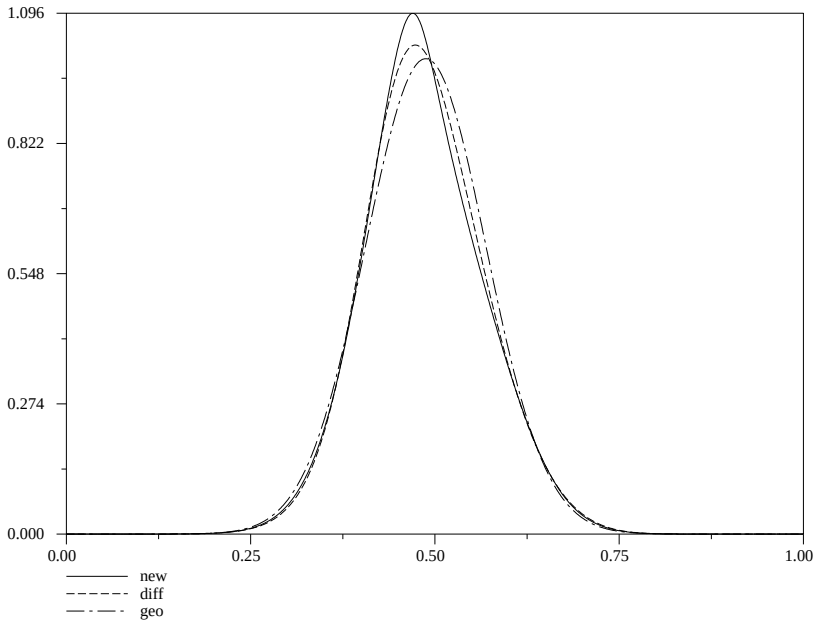

Figure 5: Amplitude of the first component of the approximate solution of (3.1) at the final time with chirped initial data, $\alpha = 0$ given by the geometrical optics, diffractive optics and new approximations, case 3.